UPPSALA
UNIVERSITET

UPTEC-ES12002
Examensarbete 30 hp
Januari 2012

LQG-control of a Vertical Axis Wind Turbine with Focus on Torsional Vibrations

Adam Alverbäck

UPPSALA
UNIVERSITET

Teknisk- naturvetenskaplig fakultet
UTH-enheten

Besöksadress:
Ångströmlaboratoriet
Lägerhyddsvägen 1
Hus 4, Plan 0

Postadress:
Box 536
751 21 Uppsala

Telefon:
018 – 471 30 03

Telefax:
018 – 471 30 00

Hemsida:
http://www.teknat.uu.se/student

Abstract

LQG-control of a vertical axis wind turbine with focus on torsional vibrations

Adam Alverbäck

In this thesis it has been investigated if LQG control could be used to mitigate torsional oscillations in a variable speed, fixed pitch wind turbine. The wind turbine is a vertical axis wind turbine with a 40 m tall axis that is connected to a generator. The power extracted by the turbine is delivered to the grid via a passive rectifier and an inverter. By controlling the grid side inverter the current is controlled and hence the rotational speed can be controlled. A state space model was developed for the LQG controller. The model includes both the dynamics of the electrical system as swell as the two mass system, consisting of the turbine and the generator connected with a flexible shaft. The controller was designed to minimize a quadratic criterion that punishes both torsional oscillations, command following and input signal magnitude. Integral action was added to the controller to handle the nonlinear aerodynamic torque.

The controller was compared to the existing control system that uses a PI controller to control the speed, and tested using MATLAB Simulink. Simulations show that the LQG controller is just as good as the PI controller in controlling the speed of the turbine, and has the advantage that it can be tuned such that the occurrence of torsional oscillations is mitigated. The study also concluded that some external method of dampening torsional oscillations should be implemented to mitigate torsional oscillations in case of a grid fault or loss of PWM signal.

Handledare: David Österberg
Ämnesgranskare: Bengt Carlsson
Examinator: Kjell Pernestål
ISSN: 1650-8300, UPTEC-ES12002

Populärvetenskaplig sammanfattning

Det här projektet har utrett ett nytt sätt att reglera ett vindkraftverk. Syftet med projektet var att utreda vilka för- och nackdelar det finns med att implementera en ny och mer avancerad regulator. Fokus låg på att studera om den nya regulatorn kan minska förekomsten av torsionssvägningar i drivaxeln.

Vindkraftverk kan antingen ha variabelt varvtal eller fast varvtal. Det vindkraftverk som har undersökts har variabelt varvtal och fast pitch. En fast pitch betyder att vingarna inte kan vridas för att optimera det aerodynamiska effektuttaget. Vindkraftverket är vertikalaxlat vilket gör att valet på fast pitch faller sig naturligt eftersom mekaniken annars skulle bli för komplicerad. Istället för att vrida på vingarna varierar vindkraftverket istället turbinens rotationshastighet för att optimera det aerodynamiska effektuttaget.

Huvudsyftet med att reglera ett vindkraftverk är att maximera effektuttaget ur vinden samtidigt som varvtalet måste begränsas inom vissa intervall. Om turbinens varvtal sammanfaller med någon egenfrekvens i vindkraftverket kan kraftiga vibrationer uppstå vilket kan leda till haveri. Dessutom finns det ett övre varvtal för vilket vindkraftverket är designat, rotationshastigheter över detta varvtal kan skapa för stora belastningar på olika komponenter med följden att de slits fortare och livslängden minskas.

Det studerade vindkraftverket använder sig av en permanentmagnetiserad synkrongenerator för att omvandla rörelseenergin till elektrisk energi som kan överföras till nätet. För att generatorn ska kunna variera sitt varvtal är den uppkopplad till nätet via en frekvensomriktare som består av en likriktare, en DC-länk och en växelriktare. Likriktaren består av sex stycken dioder, vilket betyder att den är passiv och inte kan styras. Växelriktaren, som är uppkopplad direkt mot nätet, kan däremot styra effekten som levereras till nätet och har således möjlighet att reglera den bromsande kraften på vindkraftverket.

Generatorn inducerar en spänning som är proportionell mot varvtalet. Detta medför att spänningen på DC-länken kommer att bero på generatorns varvtal. Genom att hålla spänningen på en konstant nivå kan således även varvtalet hållas på en konstant nivå. Detta utnyttjas i den nuvarande regulatorn där växelriktaren reglerar spänningen på DC-länken.

Det nuvarande styrsystemet använder sig av en PI (Proportionell, Integrerande) regulator för att hålla spänningen på rätt nivå. En PI regulator använder sig av negativ återkoppling, d.v.s. den mäter spänningen och använder det uppmätta värdet och jämför det med det referensvärde som man vill att spänningen ska ha. Differensen mellan uppmätt värde och referensvärde används sedan för att beräkna insignalen till systemet, vilket i det här fallet är strömmen ut ur växelriktaren. I det här fallet sätts referensvärdet utifrån ett 60 sekunders medelvärde av den uppmätta vindhastigheten.

Det finns vissa nackdelar och svårigheter med att reglera vindkraftverket på det sätt som beskrivits ovan. En av dessa är att effekten inte kan gå åt båda håll genom frekvensomriktaren. Detta betyder att man inte kan köra generatorn som en motor, vilket minskar reglermöjligheterna. I och med att man styr på ett 60 sekunders medelvärde av en vindhastighet som mäts 100 meter bort är det ofta svårt att ligga på optimalt varvtal. Ett annat problem är att det inte går att hitta en perfekt

referensspänning eftersom luftens densitet varierar. Detta har att göra med att varvtalet inte enbart beror på spänningen på DC-länken, utan även vilken effekt som levereras. Effekten är i sin tur direkt proportionell mot luftens densitet vilken kan variera med ungefär 20 %.

Den regulator som har tagits fram i det här examensarbetet är en så kallad LQG (Linear Quadratic Gaussian) regulator. Det är en regulator som bygger på tillståndsåterkoppling, där man istället för att endast återkoppla från en uppmätt signal, återkopplar från alla tillståndsvariabler i en modell av systemet. Regulatorn togs fram och justerades så att den klarade av ett steg i referenssignalen utan att några oscillationer uppstod. Ett Kalmanfilter anpassades för att kunna hantera störningar och för att inte försöka dämpa svängningar på ca 50 Hz som uppstår naturligt i generatorn.

Regulatorn implementerades och simulerades i en redan befintlig Simulink-modell av vindkraftverket där olika scenarior testades. Små förenklingar av modellen gjordes för att underlätta implementeringen samt för att avgränsa arbetet.

Slutsatser som man kan dra utifrån resultaten är att den nya regulatorn klarar av att styra vindkraftverket lika bra som det existerande styrsystemet. Beroende på hur regulatorn justeras kan den anpassas till att antingen klara av ett stegsvar utan vibrationer, d.v.s. långsamt stegsvar, eller så kan den justeras till att bli snabbare, med följden att vibrationer uppstår vid ett steg. Det är dock föga troligt att referenssignalen skulle ändras så snabbt under normal drift, eftersom den sätts utifrån ett 60 sekunders medelvärde av vindhastigheten.

Det finns flera olika utvecklingar av det här projektet. Till exempel skulle regulatorn kunna utvecklas och komplimenteras med ett ”Extended Kalmanfilter” för att förbättra skattningen av det aerodynamiska vridmomentet. Dessutom skulle förmodligen antalet mätsignaler kunna reduceras för att förenkla en eventuell implementering. Förmodligen är det tillräckligt att enbart mäta spänning och varvtal, eller kanske endast en av de två.

För att dämpa eventuella svängningar som uppstår i drivaxeln på grund av störningar i styrningen av växelriktaren föreslås en lösning där en extern krets kopplas till en resistiv last används för att mata ut en effekt i motfas med svängningarna. Det bör dock undersökas hur mycket en sådan lösning kan dämpa svängningarna i förhållande till den mekaniska och elektriska dämpning som redan finns i form av förluster i lager, kopplingar och elektriska kretsar.

Acknowledgments

I would like to express my greatest gratitude towards Hans Norlander at the Division of Systems and Control at Uppsala University for his time and support. I would also like to thank my supervisor, David Österberg, for reading and revising the report over and over again; Elias Björkelund, Jon Kjellin and Mats Wahl at Vertical Wind for their help with all my questions concerning the plant; Fredik Bülow at the Division for Electricity at Uppsala University for his time and encouragement; Bengt Carlsson at the Division of Systems and Control at Uppsala University for his input and Kjell Pernestål at Uppsala University for his help with administrative questions. Most of all I would like to thank my girlfriend, Lisette Edvinsson, and my study mates at the Energy systems program for their unlimited patience, support and encouragement throughout the years.

Contents

Abbreviations

- LQG - Linear Quadratic Gaussian
- IGBT - Insulated Gate Bipolar Transistor
- WECS - Wind Energy Converting System
- PMSG - Permanent Magnet Synchronous Generator
- VSFP - Variable Speed, Fixed Pitch
- VSVP - Variable Speed, Variable Pitch
- PI - Proportional, Integral
- ARE - Algebraic Riccati Equation
- DC - Direct Current
- AC - Alternating Current
- NMPC - Nonlinear Model Predictive Control
- PWM - Pulse Width Modulation
- SPWM - Sinusoidal Pulse Width Modulation

Chapter 1

Introduction

The control system of wind turbines is an ongoing area of research. One of the biggest reasons for wind turbine break downs can be derived to failure in the control system [1]. Different controllers may result in different sensitivities to disturbances. Hence it is important to compare different controllers and to look at the advantages and disadvantages.

In this thesis two similar ways of controlling a wind turbine have been compared with, special concern taken to torsional oscillations. The wind turbine under study is a vertical axis variable speed wind turbine (Figure 1.1). This kind of turbine is a variable speed fixed pitch turbine, and has to be controlled as such.

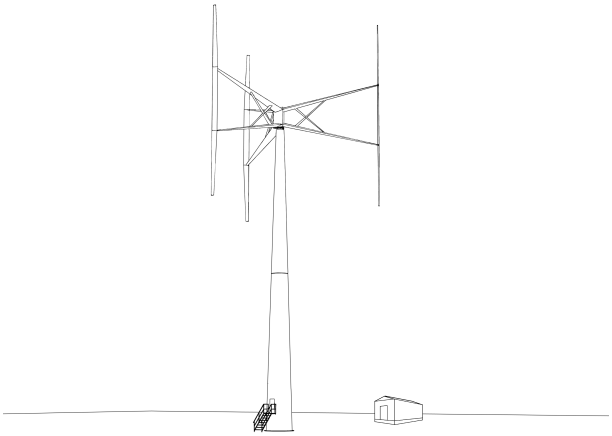

Figure 1.1: Illustration of the vertical axis wind turbine together with substation. ©Vertical Wind.

1.1 Different types of turbines

There are several different designs of wind energy converting systems (WECSs) and each design has its own optimal control strategy. Hence, it is important to distinguish them from each other. The different control strategies can be divided into different categories depending on whether or not the speed of the turbine is varying and if the wings can be pitched or not. Turbines can either be run at variable speed or at fixed speed. Fixed speed turbines have the advantage that they can be connected directly to the grid. The advantage of variable speed turbines is that the turbine can be better adapted to varying wind speeds and increase the output power.

1.1.1 Variable speed, variable pitch wind turbines

One of the most common wind turbines is the variable speed, variable pitch (VSVP) wind turbine. This type of wind turbine has blades with the possibility to be twisted during operation such that they absorb maximum power. In addition, they also have the possibility of controlling the power by varying the speed of the turbine.

1.1.2 Variable speed, fixed pitch wind turbines

Variable speed, fixed pitch (VSFP) turbines, as the one considered in this project, can only be controlled with stall regulation, by varying the speed of the turbine. The advantage is that there are less moving parts and hence less parts that can break. To have pitch control on a vertical axis wind turbine is possible but not a preferable solution. The wings would have to be twisted all over the rotational cycle and the moving parts would soon be worn out.

There has been very few studies on VSFP turbines. This can be explained by the fact that the wind turbine that has governed the market is the VSVP turbine. In many cases the control of these two types are similar for the partial load region, where the VSVP turbines keep the pitch constant and varies the rotational speed to maximize the power output.

1.2 Objective

The aim of this master thesis is to compare two different controllers for a vertical axis wind turbine. The conventional proportional integral (PI) controller is compared to Linear Quadratic Gaussian (LQG) control with special concern taken to torsional vibration suppression. The two controllers differ in one important way, the PI controller controls the rectified voltage whereas the LQG controller controls the rotational speed of the turbine.

1.3 Methods

The project was carried out in three steps:

- Literature study and modeling
- Development of controllers
- Evaluation of the control strategies using simulations

The literature study was carried of to give some insight to what has been done in the area of torsional vibrations and suggestions of solutions to the problem.

A model of the dynamical system was built that included both the dynamics of the mechanical drive train and the electrical conversion system. The model was used to tune the LQG regulator and to run some off-line simulations using MATLAB's ode solver, ode15s. The controllers were then implemented into a Simulink model to see how they would interact with the nonlinear system dynamics.

Finally some qualitative analysis was carried out in the frequency domain to compare the both controllers.

1.4 Project limits

The investigation is purely theoretical. The aim is to control the power plant by using an inverter that is connected to the grid. The inverter controls the current into the grid, which will be seen as the input signal to the system.

The reference speed is set according to a mean wind speed in both controllers, and for the PI the reference speed is converted into a reference DC (direct current) voltage.

The wind speed is only varying in strength and not in direction. The tower is not modeled as flexible, neither are the wings.

The development of the controller is limited to only make sure that the rotational speed converges to the reference speed, and to make sure that it can handle disturbances. It is not developed to improve the power output of the turbine.

1.5 Earlier work

There are several studies in the literature that tries to improve the performance of the controllers for WECSs. Most of them focuses on maximizing the power output during partial load, some focuses on limiting the load fluctuations during full load and some tries to find an optimal solution for the whole operating regime of the plant.

It is important to point out that, because of the many different design possibilities of wind turbines, only a few of the earlier studies in the area use the same type of WECS configuration. None of the studies uses the exact same configuration as the one considered here, i.e. a VSFP with a permanent magnet synchronous generator (PMSG) and diode rectification combined with a current controlled inverter. Many studies use the torque onto the generator as input signal, and then has an inner control loop for the power electronics to get the desired torque.

1.5.1 Control objectives of wind turbines in continuous operation

Wind turbines has to be controlled such that the plant does not break. There are several aspects of the control of a wind turbine and there is no dominating solution to how it should be done. First of all it is important to control the speed of the turbine such that it does not accelerate above rated speed. A too high wind speed may, for instance, cause the wings to break as a result of the centrifugal force. It is also important to avoid eigenfrequencies of the tower and other mechanical parts. Other aspects of the continuous control of a wind turbine involves maximizing the output power, limiting the power below rated and starting and stopping at cut in and cut out wind speed [2].

1.5.2 LQG controlled WECS

Earlier work has shown that the power output of a WECS can be improved by improving the regulator [3]. Many studies have been carried out where an improved regulator have been compared to a less complex one. According to [4] the LQG controller can be competitive with non-linear controllers. Especially when it comes to keeping the tip speed ratio at a constant maximum value, and compared to the PI controller.

The problem that [4] had was that the LQG could only perform well around one operational point. This problem was solved by [3] by dividing the wind into two components, one high frequent turbulent component and one low frequent seasonal component. The seasonal component was used to set an operational point around which the nonlinear system was linearized, whereas the turbulent component was used to keep the tip speed ratio at its maximum during wind gusts.

The literature offers many ways of dealing with torsional oscillations. Torsional vibration suppression could be achieved either by PI control using one feedback parameter, e.g. generator speed, or by

state space feedback, where one or more states are used in a feedback loop [5]. Also, as stated in [6], the best way to regulate the speed of a two-mass system with motor controlled speed in one end is, if possible, to use an augmented state space control .

LQG control combined with additional measurement sensors on the blades has also proven to successfully alleviate fatigue loads from bending of the blades and the tower [7, 8]. The cited studies could avoid fatigue loads by using individual pitch on each blade combined with torque control of the generator, making use of the LQG's ability to handle multiple input, multiple output problems.

One of the most important tasks of the control system is to provide a reference speed such that the tip speed ratio is kept at its maximum. This is not a trivial task because the wind speed can not be measured exactly. Hence, there is a need for estimating the wind speed or in some other way finding the reference speed, e.g. as a function of an estimation of the aerodynamic torque, as in [9]. It has been shown that the Extended Kalman filter performs well in estimating the wind speed or the aerodynamic torque [10–12].

1.5.3 Other suggested controllers

Other, nonlinear control structures, that have been suggested in the literature are: Nonlinear model predictive control (NMPC) [12], Sliding mode control [13], Nonlinear state feedback-PI controller with estimator [14] and fuzzy control [9], among others.

1.5.4 Torsional oscillations in the drive train

The phenomena with torsional oscillations in the drive train of variable speed wind turbines with frequency converters has been subject to some recent studies [15–17]. They have shown that synchronous generators with back-to-back voltage source converters are prone to give oscillations because of the lack of inherent damping. However, it turns out that all these studies used the grid side inverter to control the active power sent into the grid, and the generator side active rectifier to control the DC voltage. If instead, the grid side inverter is set to control the DC voltage, the drive train becomes stabilized with less or no oscillations [18].

Chapter 2

Theory

The drive train of the WECS consists of a 40 m tall vertical drive shaft that transmits power to the generator at ground level. The generator converts the mechanical power into electrical power that is delivered to the grid. The generator is a PMSG and because of the variable speed control strategy of the turbine, the AC (alternating current) voltage is fed to the grid via an AC/AC converter. The converter consists of a diode rectifier to convert from AC to DC, a DC bus with an inductor and a capacitor and finally a pulse width modulation (PWM) controlled inverter. The inverter is used to control the DC voltage at its reference value.

To be able to extract as much the power from the wind as possible the speed of the turbine has to be controlled. With some knowledge about the aerodynamics of the wind turbine it can be controlled such that the power output is optimized.

2.1 Aerodynamics and ideal rotational speed

The power that is extracted from the wind is given by

$$P_{turbine} = C_P \frac{1}{2} \rho A_t v^3 \tag{2.1}$$

where A_t is the projected area of the rotor facing the wind, ρ is the air density, v is the wind speed and C_P is the so called power coefficient [2]. The power coefficient describes the ratio of the energy in the free flowing wind compared to the energy that is extracted from the wind turbine and is given by

$$C_P = \frac{P_{turbine}}{P_{wind}} = \frac{P_{turbine}}{\frac{1}{2}\rho A_t v^3} \tag{2.2}$$

The ratio between the speed of the blade and the wind is called the tip speed ratio and is given by

$$\lambda = \frac{v_{blade}}{v} = \frac{\omega_t R_{turbine}}{v}$$

where ω_t is the rotational speed of the turbine and $R_{turbine}$ is the radius of the turbine. The tip speed ratio is an important number in wind turbine aerodynamics because the aerodynamic forces are dependent of that ratio, hence C_P is a function of λ. The function $C_P(\lambda)$ can be empirically estimated from aerodynamic tests but may also be calculated theoretically, as the one seen in Figure 2.1, using computational fluid dynamics.

The power that is extracted out of the wind is a function of the rotational speed of the turbine and the wind speed. The torque that is acting on the turbine from the wind is thus given by

$$T_t(\omega_t, v) = \frac{P_{turbine}}{\omega_t} = \frac{C_P(\omega_t, v)\rho A_t v^3}{2\omega_t} \tag{2.3}$$

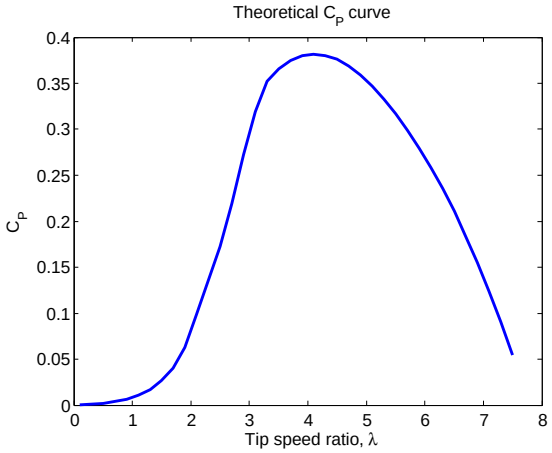

Figure 2.1: An example of how the power coefficient, C_P, depends on the tip speed ratio, λ.

The power that a wind turbine absorbs is given by equation (2.1), where C_P is the only factor that can be controlled. In Horizontal Axis Wind Turbines (HAWT) C_P can be controlled either by pitching the blades or by changing the tip speed ratio, i.e. the rotational speed of the turbine. In a Vertical Axis Wind Turbine (VAWT) it is not optimal to control the pitch of the wings, instead only the tip speed ratio is controlled.

To get the most power out of the wind C_P (Figure 2.1) is kept at its maximum value by linearly changing the rotational speed as the wind changes. When the power output becomes larger than the rated power of the plant, the tip speed ratio is decreased such that the power remains constant at its rated value. The result would be a control strategy as the one seen in Figure 2.2. The rotational speed also has to be controlled in such a way that the mechanical eigenfrequencies of the plant are avoided and to limit the mechanical loads. For this particular plant that means that the rotational speed is not allowed to be in the region of 15-18 rpm and not above 30 rpm. The maximum rotational speed is set to 30 rpm, causing the power output curve to look something like Figure 2.2 b. In winds above 25 m/s the turbine is shut down as a safety precaution.

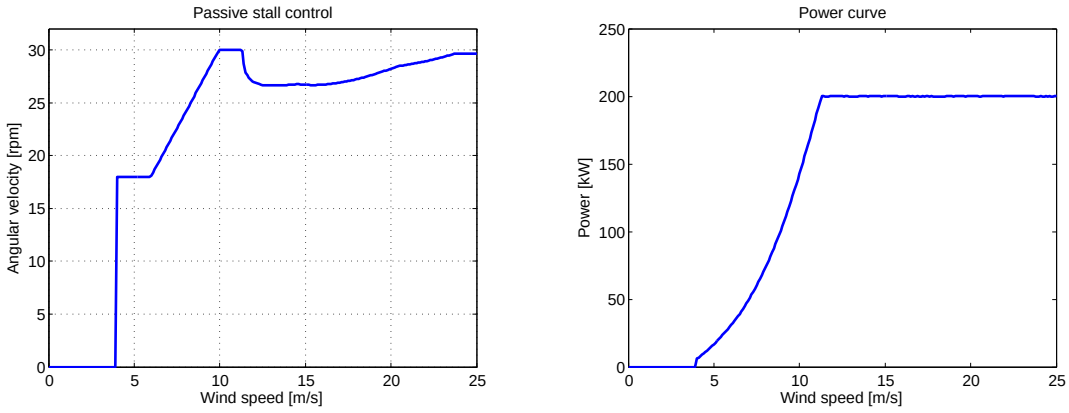

(a) Rotational speed as function of wind speed.

(b) Theoretical power curve.

Figure 2.2: Control strategy of a variable speed, fixed pitch wind turbine.

2.2 Mechanical drive train

The power that the wind turbine absorbs is transmitted to the generator through a drive shaft (Figure 2.3). The drive shaft is shaped as a cylindrical tube made of steel and can be seen as a torsional spring which starts to oscillate when the forces acting on the spring are in imbalance.

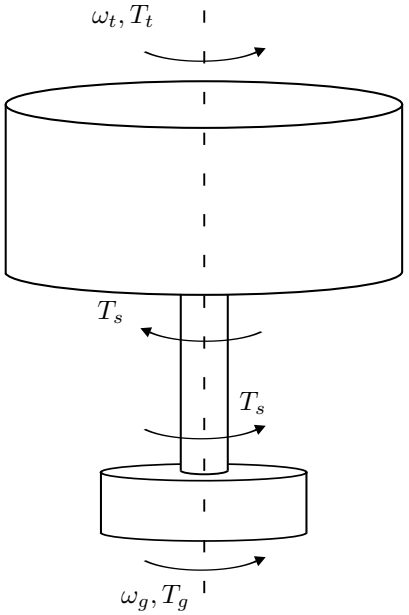

Figure 2.3: Model of mechanical system.

The two mass inertia system can be described by the equations

$$\begin{aligned} J_g\dot{\omega}_g &= T_s + T_g + D(\omega_t - \omega_g) \\ J_t\dot{\omega}_t &= T_t - T_s - D(\omega_t - \omega_g) \\ \dot{T}_s &= k_s(\omega_t - \omega_g) \end{aligned} \tag{2.4}$$

where J_g and J_t are the mass moment of inertias of the generator and the turbine, respectively, ω_g and ω_t are the rotational speeds of the generator and the turbine, respectively. T_s, T_g and T_t are the torques on the shaft, the generator and the turbine respectively (seen in figure 2.3). To describe the damping effect that arises because of the non ideal spring characteristics of the shaft a dampening torque has been added that is proportional to the difference in angular velocities with the damping parameter D, which is approximated to fit observed behavior of the shaft. The shaft stiffness, k_s, also known as the spring constant, is calculated as

$$k_s = \frac{gk}{h} \tag{2.5}$$

where h is the length of the shaft, g is the shear modulus of steel, about 79 GPa, and k is the polar moment of inertia of the shaft given as

$$k = \frac{\pi}{2}(r_1^4 - r_2^4)$$

where r_1 is the outer radius and r_2 is the inner radius of the cylinder [19].

The eigenfrequency of the spring can be calculated from

$$\omega_n = \sqrt{\frac{k_s}{J_{tot}}}$$

where J_{tot} is the resulting mass moment of for the two oscillating masses, given by

$$J_{tot} = \left(\frac{1}{J_g} + \frac{1}{J_t}\right)^{-1}$$

In equation (2.4) it is assumed that the inertia of the shaft can be neglected. However, it turns out that the inertia of the shaft is about 20 % of the inertia of the generator and should not be neglected. Instead it will be considered as a point mass in each end of the spring, i.e. half of the inertia will be added to the generator and half will be added to the turbine.

2.3 Electrical System

The electrical system consists of a permanent magnet synchronous generator to convert the mechanical power into electrical power. Because the generator is a synchronous machine and the wind turbine is a variable speed machine the voltage has to be converted to be in phase with the electrical grid. This is done via a voltage source converter consisting of a six pulse diode bridge, a DC-line and a DC/AC inverter (figure 2.4). The diode bridge rectifies the three phase AC voltage such that it becomes DC. The DC voltage can then be switched back to AC, but with a different frequency, using insulated gate bipolar transistors (IGBTs) in the inverter.

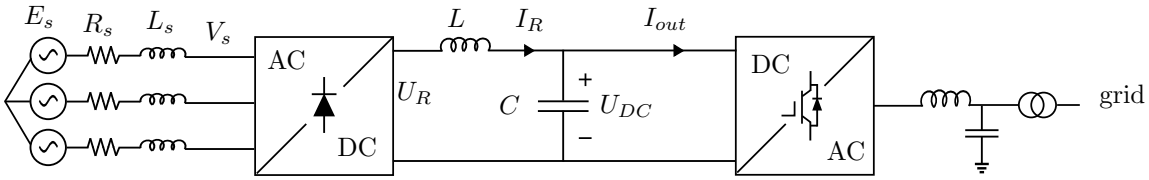

Figure 2.4: Overview of the electrical system.

The output voltage of a six pulse rectifier has the shape of a DC-voltage with six humps over one electrical cycle. The reason for that can be seen in Figure 2.5 where the output of the six pulse diode bridge is depicted as the maximum of the modulus of the three phase line-to-line input voltage.

Also the inverter causes some voltage ripple but the harmonics of that are of a much higher order and with a much higher amplitude. To keep a decent DC-voltage a low pass filter is added to the DC-line in the shape of an inductance and a capacitance. The inverter is a two-level three phase inverter that is controlled through Sinusoidal Pulse Width Modulation (SPWM) [20]. The inverted voltage is connected to the grid through a low pass LC-filter.

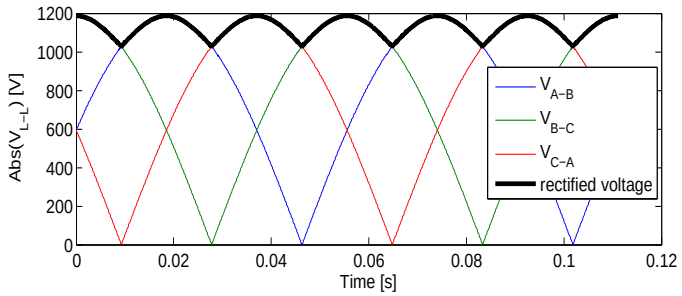

Figure 2.5: Input and output voltage of a six pulse rectifier

2.3.1 Dynamics of the electrical system

The three phase generator combined with the voltage source converter is a nonlinear system, i.e. it cannot be described by a system of linear differential equations. However, the rectified three phase voltage source can be simplified as a DC voltage source with some voltage ripple (Figure 2.6).

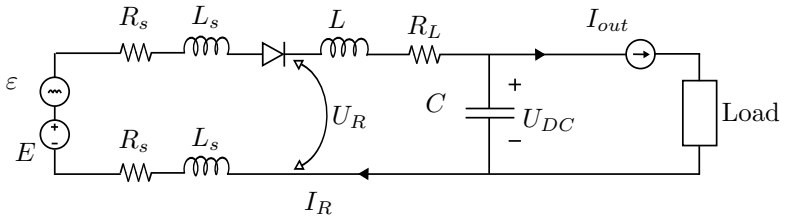

Figure 2.6: Simplified view of the electrical system, where the three phase generator has been replaced with a DC-voltage source and a voltage ripple (ε).

It can be shown that the no load rectified voltage, seen in Figure 2.5, of a three phase generator can be expressed as

$$E_R = \Lambda\omega_g\sqrt{3}\cos(\omega_{el}t - \frac{\pi}{3}); \quad \frac{\pi}{6} \leq \omega_{el}t \leq \frac{\pi}{2} \tag{2.6}$$

where Λ is the magnetic flux linkage of the generator and ω_{el} is the electrical frequency on the generator side, given as

$$\omega_{el} = N_{PP}\omega_g$$

where N_{PP} is the number of pole pairs of the generator. Equation (2.6) can be approximated as

$$E_R \approx \Lambda\omega_g\left(\frac{3}{2} + (\sqrt{3} - \frac{3}{2})|\sin(3\omega_{el}t)|\right) \tag{2.7}$$

E_R can now be written as

$$E_R = E_{DC} + \varepsilon \tag{2.8}$$

where

$$E_{DC} = \frac{3}{2}\Lambda\omega_g$$

and where ε, described as a voltage disturbance in Figure 2.6, is given by

$$\varepsilon = \Lambda\omega_g(\sqrt{3} - \frac{3}{2})|\sin(3\omega_{el}t)|$$

The equations that describe the dynamics of the electrical model depicted in Figure 2.6 can be derived from Kirchoff's laws as

$$\begin{aligned} \frac{dU_{DC}}{dt} &= \frac{1}{C_{DC}}(I_R - I_{out}) \\ E_{DC} + \varepsilon &= (2R_s + R_L)I_R + (2L_s + L_{DC})\frac{dI_R}{dt} + U_{DC} \\ I_R &\geq 0 \end{aligned} \tag{2.9}$$

where R_s and L_s are the per phase inner resistance and inductance, respectively, of the synchronous generator, L_{DC} is the inductance on the DC-line and C_{DC} is the capacitance of the DC-line. R_L is a resistance that has been added to the circuit to get a more accurate model. Equation (2.9) can be rewritten as

$$\begin{aligned} C_{DC}\dot{U}_{DC} &= (I_R - I_{out}) \\ L_{tot}\dot{I}_R &= -U_{DC} - R_{tot}I_R + E_{DC} + \varepsilon \\ I_R &\geq 0 \end{aligned} \tag{2.10}$$

where L_{tot} is the sum of the inductances and R_{tot} is the sum of the resistances in Figure 2.6.
The electrical system is linked to the mechanical system through the electrical torque given by

$$T_g = \frac{E_R I_R}{\omega_g} = \Lambda I_R \left(\frac{3}{2} + (\sqrt{3} - \frac{3}{2}) |\sin(3\omega_{el} t)| \right)$$

which can written as

$$T_g = \frac{3}{2} \Lambda I_R + \tau_g \tag{2.11}$$

where

$$\tau_g = \Lambda I_R (\sqrt{3} - \frac{3}{2}) |\sin(3\omega_{el} t)|$$

2.4 Sources of oscillations

The oscillations are excited by changes in the torque on either the turbine or the generator. As can be seen in the Bode plot (Figure 2.7) torsional oscillations are most excited through oscillations in the torque from the generator. The ratio between the inertia of the turbine and the generator is about 185. Because of the large inertia ratio the only mass that will oscillate is the generator and not the turbine, i.e. torsional oscillations are unlikely to be excited by rapid changes in the wind.

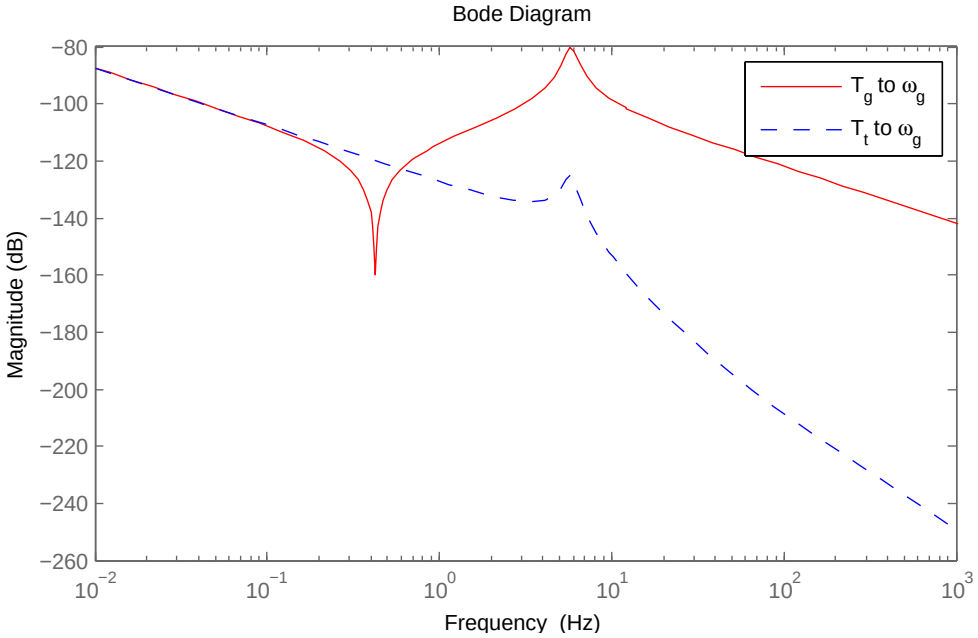

Figure 2.7: Bode diagram of mechanical drive train with a damping factor of $D = 10000$ Nm/(rad·s). From T_g to ω_g (red solid line), and from T_t to ω_g (blue dotted line).

The most likely cause for eigenoscillations to occur in the drive shaft is when the DC-voltage raises too fast. This has the consequence that the torque onto the generator will decrease too fast and the generator will start to oscillate. There could be several reasons for the DC-voltage to increase fast. One of those are that the reference voltage increases too fast for some reason, e.g. to accelerate through eigenfrequencies of the tower. It is also possible that there are disturbances on the control signal, i.e. the current into the grid. Such disturbances could either be a grid fault, or problems with the current controller.

The six pulse diode bridge causes the currents in the generator to vary as pulses with a frequency of six times the oscillating frequency. This causes a small torque ripple on the generator with the frequency of six times the electrical frequency. However, because the natural frequency of the torsional spring, i.e. the shaft, is much lower than six times the electrical frequency, even when operating at very low speeds, the torque ripple does not cause any dangerous oscillations.

There are other aspects of the generator that has not been included in the reasoning above. It all comes down to interactions of the magnetic fields between the stator and the rotor. The design of the generator and losses in the stator core may cause subharmonics to occur but these are of a few order greater than the fundamental frequency of the AC-voltage on the generator side and will only cause very small oscillations.

Chapter 3

The existing control system

The power that the turbine absorbs is regulated through passive stall control. This means that the power that is being absorbed is controlled by changing the rotational speed and hence also the tip speed ratio, λ. In other words, the turbine is a variable speed stall regulated turbine. The rotational speed is almost directly proportional to the rectified voltage and hence the rectified voltage is used as a control signal instead of the rotational speed. The voltage over the DC-line is controlled by changing the output current through the IGBT inverter (Figure 3.1).

3.1 Control structure

As can be seen in Figure 2.2 it is desirable to control the rotational speed of the turbine. This is done by letting the grid side converter control the voltage over the DC-line. By keeping the voltage at a certain level the generator will find a steady state rotational speed that corresponds to the DC-voltage. Depending on the control strategy to be used a DC-lookup table can be designed such that the rotational speed of the turbine adopts its desired value for a given wind speed. Because of the fluctuating nature of the wind the regulator is controlling the DC-voltage according to a 60 s running mean of the wind speed.

The DC/AC inverter is used both for controlling the DC-voltage at its reference value and for controlling the reactive power output. This is done through the parameters i_d and i_q, that corresponds to the grid side three phase currents' Park transformation. By using the Park transformation in a reference frame that is oriented along the grid side voltage the active and reactive power out of the converter can be written as

$$P_{grid} = \frac{3}{2} u_d i_d \tag{3.1}$$

$$Q_{grid} = \frac{3}{2} u_d i_q \tag{3.2}$$

where u_d is the Park transformation d-component of the three phase grid voltage [21]. This implies that the DC-current can be controlled through the i_d component and that the reactive power can be controlled through the i_q component. The inverter cannot be controlled to give a direct value of the i_d and i_q components. Instead it utilizes a current controller as to make sure that the inverter produces the correct current.

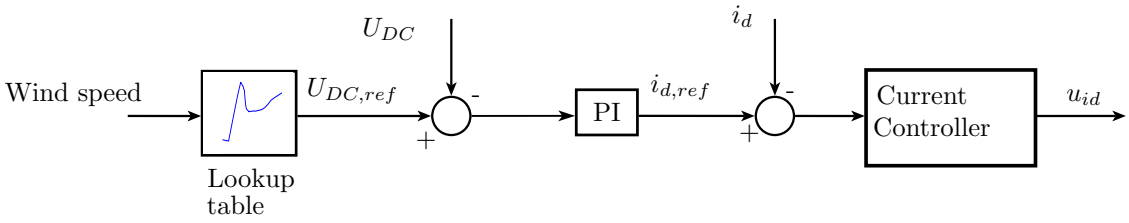

Figure 3.1: Model of the present control mechanism.

3.2 Current controller

The equations that govern the dynamics of the inverter are given by

$$\begin{aligned} u_{id} &= u_d + R_{grid} i_d + L_{grid} \frac{di_d}{dt} - \omega_{grid} L_{grid} i_q \\ u_{iq} &= u_q + R_{grid} i_q + L_{grid} \frac{di_q}{dt} + \omega_{grid} L_{grid} i_d \end{aligned} \tag{3.3}$$

where u_{id}, u_{iq} represent the inverter voltage, u_d, u_q represent the grid voltage, ω_{grid} is the electrical frequency of the grid and L and R are the grid inductance and resistance, respectively [21]. Equation (3.3) can not be implemented directly because the exact load of the grid would have to be known. Instead it is implemented as a PI controller with two feedforward terms (Figure 3.2) [20].

Once u_{id} and u_{iq} have been decided they are transformed back into three phase voltages and sent to the SPWM that translates the voltages into pulses for the IGBT inverter [20]. The voltage that is sent to the SPWM represents the so called modulation index. The relationship between the modulation index and the voltages is that the grid side phase rms-voltage is given by

$$U_{a,b,c} = \frac{1}{\sqrt{3}\sqrt{2}} m_a U_{DC}$$

where m_a is the amplitude modulation index [21]. Hence the voltages u_{id} and u_{iq} has to be converted into per units of the DC-voltage. It should be pointed out that this method of controlling the inverter works best if the DC-voltage is kept at a constant value, which is not the case in this type of converter setup.

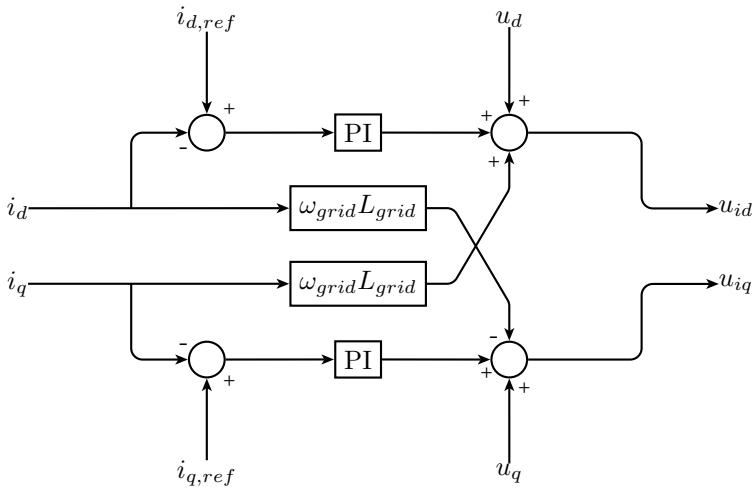

Figure 3.2: The current control system for the inverter.

The inverter can make the current go both into the grid from the DC-line and out of the grid into the DC-line. The advantage of this is that the generator do not have to feed the capacitors with

energy when the turbine is supposed to accelerate, instead energy can be taken from the grid. This allows the generator to accelerate faster. The drawbacks of this is that when the DC-voltage reaches above the no-load voltage of the generator it will not deliver any power and hence there will be no torque on the generator and the rotational speed cannot be controlled. This causes the generator to oscillate because there is no torque that can force it to stay in position.

Chapter 4

Suggestion of a new control system

In the literature there are at least two different ways to handle the torsional vibration problem, depending on the type of problem and the sources of oscillations. One solution origins from the wind power industry as a way to deal with torsional vibrations of the drive shaft in a wind turbine. The idea is to let the DC-side voltage vary such that a torque that oscillates off phase with the torsional vibrations is induced in the generator [15,16]. The other solution origins from the automatic control area and is based on the idea of state space feedback and the theory of LQG-control [22].

The main idea with LQG-control is to make use of all the states in a state space model to control the behavior of the system. The theory assumes that the system can be modeled as a linear system of differential equations as

$$\begin{aligned} \dot{x} &= Ax + Bu + Nv_1 \\ y &= Cx + v_2 \end{aligned} \tag{4.1}$$

where x is the state vector, u is the input signal, y is the measured output signal, and v_1 and v_2 are white noises [23]. The matrices A, B and N define the system of equations and C defines which states that are measured. In the new control system it is assumed that measured input signals into the controller are the rotational speed of the generator, ω_g, the current out of the rectifier, I_R, and the voltage across the capacitor, U_{DC}. The output of the regulator is the same as in the existing control system, i.e. the DC-current fed into the grid, I_{out}.

4.1 The state space model

The mechanical drive train can be modeled as described by equations (2.4), where the damping coefficient is approximated to fit observed behavior of the shaft and the shaft stiffness parameter is calculated as in equation (2.5). The torque from the air is modeled as

$$T_t = T_t(\omega_t, v) + \Delta T_t \tag{4.2}$$

where $T_t(\omega_t, v)$ is the torque onto the turbine from the wind according to equation (2.3) and ΔT_t is some integrated white noise, w, describing the model errors in $T_t(\omega_t, v)$.

Equations (2.4) and (4.2) are combined with equation (2.10) to include the dynamics of the electrical

system into the model. The result is a system of differential equations given as

$$\begin{aligned} J_g\dot{\omega}_g &= T_s - \frac{3}{2}\Lambda I_R + D(\omega_t - \omega_g) - \tau_g \\ J_t\dot{\omega}_t &= T_t(\omega_t, v) + \Delta T_t - T_s - D(\omega_t - \omega_g) \\ \dot{T}_s &= k_s(\omega_t - \omega_g) \\ C_{DC}\dot{U}_{DC} &= (I_R - I_{out}) \\ L_{tot}\dot{I}_R &= -U_{DC} - R_{tot}I_R + \frac{3}{2}\Lambda\omega_g + \varepsilon \\ \Delta\dot{T}_t &= -\delta\Delta T_t + w \end{aligned} \tag{4.3}$$

where δ is a small scalar that has been added to make sure that the system can be stabilized. To fulfill the model (4.3), two constraints are added to describe the effect of the diode in Figure 2.6 and the fact that the DC-voltage cannot be lower than the grid side voltage:

$$\begin{aligned} U_{DC} &\geq U_{grid} \\ I_R &\geq 0 \end{aligned}$$

where U_{grid} is the peak, line-to-line voltage of the grid.

With state variables chosen as

$$x = \begin{bmatrix} \omega_g & \omega_t & T_s & U_{DC} & I_R & \Delta T_t \end{bmatrix}^T$$

the system of differential equations (4.3) can be written

$$\dot{x} = Ax(t) + BI_{out} + ET_t(\omega_t, v) + \Psi \begin{bmatrix} \tau_g \\ \varepsilon \end{bmatrix} + \begin{bmatrix} 0 \\ 1 \end{bmatrix} w \tag{4.4}$$

where

$$A = \begin{bmatrix} -D/J_g & D/J_g & 1/J_g & 0 & -1.5\Lambda/J_g & 0 \\ D/J_t & -D/J_t & -1/J_t & 0 & 0 & 1/J_t \\ -k_s & k_s & 0 & 0 & 0 & 0 \\ 0 & 0 & 0 & 0 & 1/C_{DC} & 0 \\ 1.5\Lambda/L_{tot} & 0 & 0 & -1/L_{tot} & -R_{tot}/L_{tot} & 0 \\ 0 & 0 & 0 & 0 & 0 & -\delta \end{bmatrix}$$

$$B = \begin{bmatrix} 0 & 0 & 0 & -1/C_{DC} & 0 & 0 \end{bmatrix}^T$$

$$E = \begin{bmatrix} 0 & -1/J_t & 0 & 0 & 0 & 0 \end{bmatrix}^T$$

$$\Psi = \begin{bmatrix} 1/J_g & 0 & 0 & 0 & 0 & 0 \\ 0 & 0 & 0 & 0 & 1/L_{tot} & 0 \end{bmatrix}^T.$$

4.2 Configure the complimentary sensitivity function

Here it is described how the regulator is made less sensitive to the fast vibrations in the generator that arises as a consequence of the rectification.

The six pulse rectification will cause the voltage, current and generator to vibrate with a high frequency ($6\omega_{el}$). The input signal cannot be controlled to vary fast enough such that these vibrations are damped, nor is that the purpose with the suggested regulator. It is supposed to damp eigenoscillations with the frequency of about 5 Hz. Hence the regulator has to be made less sensitive to vibrations with the frequency of six times the electrical frequency. This is done by adding a filtered white noise to the measurement such that the Kalman filter would treat the oscillations of $6\omega_{el}$ as measurement noise.

Another way to put it is to say that the measurement noise is given a lot of energy at the frequencies that should be filtered out by the Kalman filter. In that way the complimentary sensitivity function will be very small for those frequencies.

A transfer function that is suitable for this purpose is

$$\Pi(s) = \frac{1}{s^2 + 0.01s + (6N_{pp} \cdot 2.8)^2}$$

which is a second order transfer function, hence two more states has to be added to the system of equations, for each filter. The second order transfer function is converted into state space with controller canonical form. For the sake of simplicity only two of the three measured signals will be filtered, chosen as ω_g and I_R. The new augmented A matrix can be written

$$A_b = \begin{bmatrix} A & 0 & 0 \\ 0 & a & 0 \\ 0 & 0 & a \end{bmatrix}$$

and the measured output states are expressed as

$$y = Cx_b + v_2$$

where

$$a = \begin{bmatrix} -0.01 & -(6N_{pp} \cdot 2.8)^2 \\ 1 & 0 \end{bmatrix}$$

and

$$C = \begin{bmatrix} 1 & 0 & 0 & 0 & 0 & 0 & 0 & 1 & 0 & 0 \\ 0 & 0 & 0 & 0 & 1 & 0 & 0 & 0 & 0 & 0 \\ 0 & 0 & 0 & 0 & 0 & 1 & 0 & 0 & 0 & 1 \end{bmatrix}$$

and where

$$x_b = \begin{bmatrix} x & \dot{\tau}_g & \tau_g & \dot{\varepsilon} & \varepsilon \end{bmatrix}^T$$

The expanded version of equation (4.4) is then written as

$$\begin{aligned} \dot{x}_b &= A_b x_b + B_b I_{out} + E_b T_t(\omega_t, v) + N v_1 \\ y &= C x_b + v_2 \end{aligned} \tag{4.5}$$

where v_1 and v_2 are white noise disturbances with covariance R_1 and R_2, respectively. The term Nv_1 has been added to describe model errors and other process noises that may exist and the term v_2 describes the measurement noise.

4.3 State space feedback and Kalman filter

The advantage of using state space feedback for controlling the wind power plant is that more than one state can be used in the feedback loop, and hence there are more opportunities to control the behavior of the plant. The drawback is that not all the states are measurable, in this case only ω_g, U_{DC} and I_R are measurable. The other states has to be estimated by using an observer.

Let $\hat{x}_b$ denote the estimated value of the state vector x_b. This can be estimated from the knowledge of the physical system (4.5) combined with a Kalman filter to filter out white noise disturbances as

$$\dot{\hat{x}}_b = A_b \hat{x} + B_b I_{out} + E_b T_t(\hat{\omega}_t, v) + K(y - C\hat{x}) \tag{4.6}$$

where K, known as the Kalman filter gain, is given by

$$K = (PC^T + NR_{12})R_2^{-1}$$

where P is the positive semi-definite solution to the algebraic Riccati equation (ARE)

$$A_b P + P A_b^T + N R_1 N^T - (P C^T + N R_{12}) R_2^{-1} (P C^T + N R_{12})^T = 0$$

where R_1 and R_2 are the intensities of v_1 and v_2, in equation (4.5), respectively. R_{12} is the cross covariance of v_1 and v_2, and will be neglected [23].

Here R_1, N and R_2 are chosen as

$$N = \begin{pmatrix} 1 & & \dots & & 0 \\ & 0 & & & \\ & 1 & & & \\ & & 1 & & \\ \vdots & & & 1 & \vdots \\ & & & & 1 \\ & & & & 0 \\ & & & & & 1 \\ 0 & & \dots & & 0 \end{pmatrix} \quad R_1 = \begin{pmatrix} 1 & & \dots & & 0 \\ & 1 & & & \\ & & 10^8 & & \\ \vdots & & & 10^8 & \vdots \\ & & & & 10^2 \\ & & & & & 10^8 \\ 0 & & \dots & & 10^{24} \end{pmatrix}$$

$$R_2 = \begin{pmatrix} 10^{-3} & 0 & 0 \\ 0 & 10^{-1} & 0 \\ 0 & 0 & 10^{-1} \end{pmatrix}$$

and R_{12} was set to zero.

To get a good estimation of $\hat{x}$, the Kalman filter should be calculated from a linear description of the system. The torque from the air, $T_t(\omega_t, v)$, is a nonlinear function (Figure 4.1 a), and is linearized to be included in the Kalman filter. The function is linearized in four sections (Figure 4.1 b) such that four different Kalman filters can be calculated, one for each section. The linearized representation $T_t(\omega_t, v)$ is given by the Taylor expansion

$$T_t(\omega_t, v) = T_t(\omega_{t,0}, v_0) + \frac{\partial T_t}{\partial \omega_t}(\omega_t - \omega_{t,0}) + \frac{\partial T_t}{\partial v}(v - v_0)$$

around four different points $(\omega_{t,0}, v_0)$.

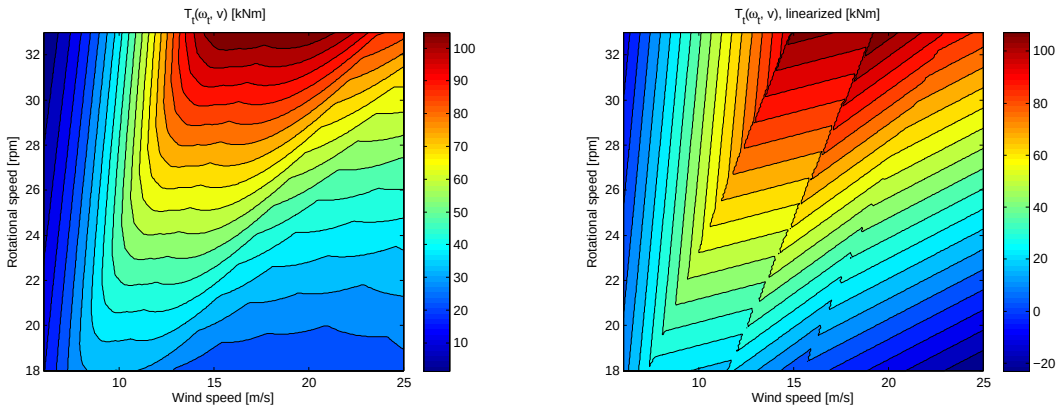

(a) Theoretical, nonlinear function.

(b) Piece-wise linearized function.

Figure 4.1: The torque dependence of the rotational speed of the turbine and the wind speed.

4.4 Adding integral action

Adding integral action to the controller is a way to make sure that the steady-state error goes to zero [22]. To include integral action into the controller a new state variable is defined as

$$\epsilon(t) = \int_0^t (\omega_t - \omega_{ref}) d\tau \tag{4.7}$$

The time derivative of equation (4.7) is added to equation (4.5) to form an augmented state space model

$$\begin{bmatrix} \dot{x} \\ \dot{\epsilon} \end{bmatrix} = \begin{bmatrix} A_b & 0 \\ M & 0 \end{bmatrix} \begin{bmatrix} x \\ \epsilon \end{bmatrix} + \begin{bmatrix} B_b \\ 0 \end{bmatrix} I_{out} + \begin{bmatrix} E_b & 0 \\ 0 & -1 \end{bmatrix} \begin{bmatrix} T_t \\ \omega_{ref} \end{bmatrix} \tag{4.8}$$

where

$$M = \begin{bmatrix} 0 & 1 & \dots & 0 \end{bmatrix}_{1 \times n}$$

where n is the dimension of A_b.

If it is assumed that the system (4.8) is stable it can be rewritten as the deviation from a steady state state point, x_s, as

$$\dot{z} = A_c z + B_c q \tag{4.9}$$

where

$$A_c = \begin{bmatrix} A_b & 0 \\ M & 0 \end{bmatrix} \quad B_c = \begin{bmatrix} B_b \\ 0 \end{bmatrix}$$

and

$$z = \begin{bmatrix} x - x_s \\ \epsilon - \epsilon_s \end{bmatrix} \tag{4.10}$$

and the input signal, q, is

$$q = I_{out} - I_{out,s} \tag{4.11}$$

where x_s, ϵ_s and $I_{out,s}$ stands for the steady-state point of the corresponding variable [22].

The state feedback law for the system (4.9) is given by

$$q = -Lz \tag{4.12}$$

where L is the state space feedback vector. By substituting for equations (4.10) and (4.11) into equation (4.12), it can also be written as

$$I_{out} - I_{out,s} = -L \begin{bmatrix} x - x_s \\ \epsilon - \epsilon_s \end{bmatrix}$$

The steady state terms must cancel out and, according to [22], the state feedback law (4.12) becomes

$$I_{out} = -L \begin{bmatrix} x \\ \epsilon \end{bmatrix} \tag{4.13}$$

4.5 Finding the optimal controller

The main idea with LQ-theory is to find a regulator that minimizes a quadratic criterion. To penalize both torsional vibrations and the control error the criterion to be minimized is chosen as

$$\begin{aligned} J = \int_0^\infty \big(& \alpha(\omega_g - \omega_t)^2 + \beta(\omega_t - \omega_{ref})^2 \\ & + \gamma(\epsilon - \epsilon_s)^2 + Q_2(I_{out} - I_{out,s})^2 \big)\, dt \end{aligned} \tag{4.14}$$

where α, β, γ and Q_2 are parameters for penalizing torsional vibrations, command following, steady-state error and the control input, respectively.

Equation (4.14) can be written as

$$J = \int_0^\infty \left(z^T Q_1 z + q^2 Q_2 \right) dt \tag{4.15}$$

where z is the state vector given by equation (4.10), Q_1 is a matrix to penalize the states and Q_2 is a scalar to penalize the control input. Q_1 is given as

$$Q_1 = \begin{bmatrix} \alpha & -\alpha & \dots & 0 \\ -\alpha & \alpha+\beta & \dots & 0 \\ \vdots & \vdots & 0 & \vdots \\ 0 & 0 & \dots & \gamma \end{bmatrix}_{n \times n}$$

where n is the dimension of A_c.

LQG-theory states that the regulator that minimizes the criterion (4.15) is given by the control law (4.12) or equivalently (4.13)

$$I_{out} = -L \begin{bmatrix} x \\ \epsilon \end{bmatrix}$$

where L is the state feedback vector which, according to [23], is given by

$$L = Q_2^{-1} B_c^T S$$

where S is the positive semi-definite solution to the ARE

$$A_c^T S + S A_c + Q_1 - S B_c Q_2^{-1} B_c^T S = 0.$$

4.6 Discrete representation

Once the system has been modeled in the continuous time domain it has to be converted into a system of discrete difference equations. This is to make it possible to implement the regulator in a digital control system. The transformation to discrete time can be made with different methods. The Zero Order Hold (ZOH) method has been chosen in this case. The discrete representation of equation (4.5) is thus written as

$$\begin{aligned} x_{k+1} &= F x_k + G I_{out,k} + H T_{t,k} + \xi v_1 \\ y_k &= C x_k + v_2 \end{aligned} \tag{4.16}$$

where

$$F = e^{A_b T} \tag{4.17}$$

where T is the sampling period. The other matrices are calculated as

$$\begin{bmatrix} G & H & \xi \end{bmatrix} = \int_0^T e^{A_b t} dt \begin{bmatrix} B_b & E_b & N \end{bmatrix} \tag{4.18}$$

where the exponential of a matrix is given as

$$e^{A_b t} = \mathcal{L}^{-1}\{(sI - A_b)^{-1}\}$$

The disturbances, v_1 and v_2, are now seen as discrete and their continuous covariance matrices, R_1 and R_2, have to be converted into their discrete equivalents. According to [24] this is done as

$$\begin{aligned} R_{1,d} &= \int_0^T e^{A_b t} G R_1 G^T e^{A_b^T t} dt \\ R_{2,d} &= R_2 / T. \end{aligned} \tag{4.19}$$

The discrete version of equation (4.6) becomes

$$\hat{x}_{k+1} = F\hat{x}_k + GI_{out,k} + HT_t(\hat{\omega}_{t,k}, v_k) + K(y_k - C\hat{x}_k) \tag{4.20}$$

where K is given by

$$K = (FPC^T + \xi R_{12,d})(CPC^T + R_{2,d})^{-1}$$

where P is the positive semi-definite solution to the discrete ARE

$$FPF^T + \xi R_{1,d}\xi^T - (FPC^T + \xi R_{12,d})(CPC^T + R_{2,d})^{-1}(FPC^T + \xi R_{12,d})^T = P.$$

Because the state ϵ is fictitious it is not included in the calculations of the Kalman filter. The discrete integrated control error is calculated as

$$\epsilon_{k+1} = \epsilon_k + (\hat{\omega}_{t,k} - \omega_{ref})T.$$

The discrete LQ-regulator is given as

$$I_{out,k} = -L \begin{bmatrix} \hat{x}_k \\ \epsilon_k \end{bmatrix}$$

where the feedback vector, L, is computed as

$$L = (G_c^T S G_c + Q_2)^{-1} G_c^T S F_c$$

where S is the positive semi-definite solution to the discrete ARE

$$F_c^T S F_c + Q_1 - F_c^T S G_c (G_c^T S G_c + Q_2)^{-1} G_c^T S F_c = S$$

where the discrete equivalents of A_c and B_c have been used. These are given as

$$F_c = e^{A_c T} \quad G_c = \begin{bmatrix} G \\ 0 \end{bmatrix}.$$

4.7 Software

The Kalman filter and LQ controller were calculated with the help of the control system toolbox in MATLAB. The continuous system was converted into a discrete system using the function `c2d(contsys, dt)`. The discrete LQ controller was calculated using the function `LQRD`. The discrete Kalman filter was calculated with the function `KALMD`.

`LQRD` uses `c2d` and then the command `DLQR`, which is the same as solving the discrete ARE. `KALMD` first discretizes the system and the covariance matrix according to equations (4.16) -(4.19), then uses `DLQE` to get the discrete Kalman filter.

Chapter 5

Simulations and results

The controllers were implemented in MATLAB Simulink together with a detailed model. This would give a good idea of how they would work in reality and how they would handle different scenarios. They were also simulated in a simplified linear version of the model, without limitations. This simulation was carried out using the MATLAB function `ode15s`, a differential equation solver for stiff problems. The advantage of using the simplified linear model is that the simulations run a lot faster and gives an idea of the behavior of the regulator. By using the linear model the LQ-controller could be tuned, the PI controller was already tuned and, as such, the linear model could only be used to give an idea of the behavior of it.

5.1 Simulink model

The Simulink model that was used for evaluation of the two controllers was a detailed model, previously developed by Vertical Wind. The model was slightly modified to fit within the boundaries of this project. The simplification was that the inverter, that controls the current, and the grid were replaced by a current source and a resistive load. The model that was used included a wind and turbine model, a mechanical model and an electrical model of the generator, the rectifier and the DC-line.

5.1.1 Wind and turbine model

The wind was modeled as filtered white noise around some user defined mean wind. The filter was designed such that the covariance and probability function of the wind speed became realistic. The wind direction was not modeled. This should not affect the result because the torque on the turbine does not depend on the wind direction, since the vertical axis turbine absorbs winds from every direction.

The torque on the turbine from the wind was modeled as $T_t(\omega_t, v)$, as in equation (2.3), with some torque fluctuations added. The torque fluctuations describe the fact that the wings experience a varying torque over one cycle as a consequence of the varying angle of attack.

5.1.2 Mechanical and electrical model

The shaft was modeled as a torsional spring without inertia but with damping, i.e. equation (2.4). The shaft was implemented as a state space equation with the aerodynamic torque onto the turbine and the electrical torque onto the generator as input signals.

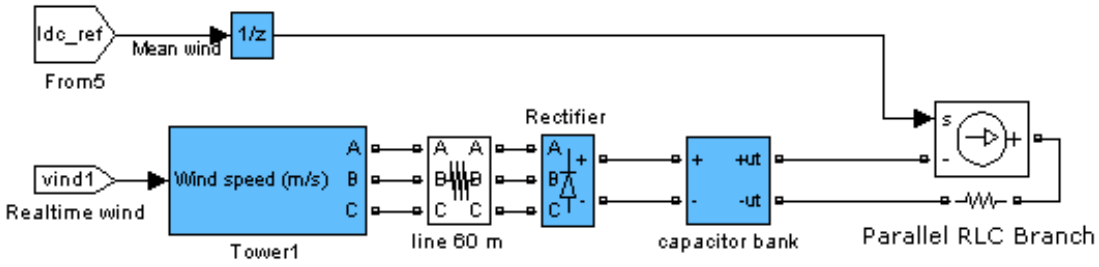

Figure 5.1: Overview of the Simulink model used for time domain simulations. For a more detailed view, see appendix.

The generator was included into the model as a component from the Sim Power Systems toolbox. The generator model takes the rotational speed as input and calculates the torque and the three phase terminal voltage of the generator. The voltage can either be modeled as trapezoidal or sinusoidal, here it was modeled as a trapezoidal voltage. Also the model of the electrical system, including the six pulse rectifier, the DC-line and the current source were added to the model as blocks from the Sim Power Systems toolbox (Figure 5.1).

5.1.3 Model limitations

The model does not take grid variations into account, such as voltage dips or grid faults. Grid variations may be one of the greatest sources of disturbances. In the simulations such disturbances were simply considered as disturbances on the output current, I_{out}.

The mechanical model of the shaft does not take the nonlinear behavior of the shaft into account. The shaft is divided into two parts connected like coggings in the middle. Because of the small spacing between the parts they hit each other whenever the torque in the shaft switches sign. This hit sounds like a big ”clonk” and should probably have a dampening effect on the vibrations of the shaft.

5.2 Frequency response

To compare the two control strategies one can look at the response to different signals in the frequency domain. The frequency response is only validated by using the linear model, equations (4.3), without any constraints or disturbances, using the continuous time regulator. By doing so, one can get a good idea of how the system will behave in case of different disturbances.

5.2.1 Closed loop

The frequency response of the closed loop of the two controllers can be seen in Figures 5.2 and 5.3. Figure 5.2 shows that there is a peak at 9 Hz for the PI controller, indicating that there could be some oscillations using this regulator. As can be seen in Figure 5.3 there is no peak, indicating that the LQG controller does not cause oscillations when the reference signal is changed.

5.2.2 Input sensitivity function

The input sensitivity function for the two controllers can be seen in Figure 5.4. It is a measure of how the control system reacts to a disturbance on the input signal, i.e. I_{out}.

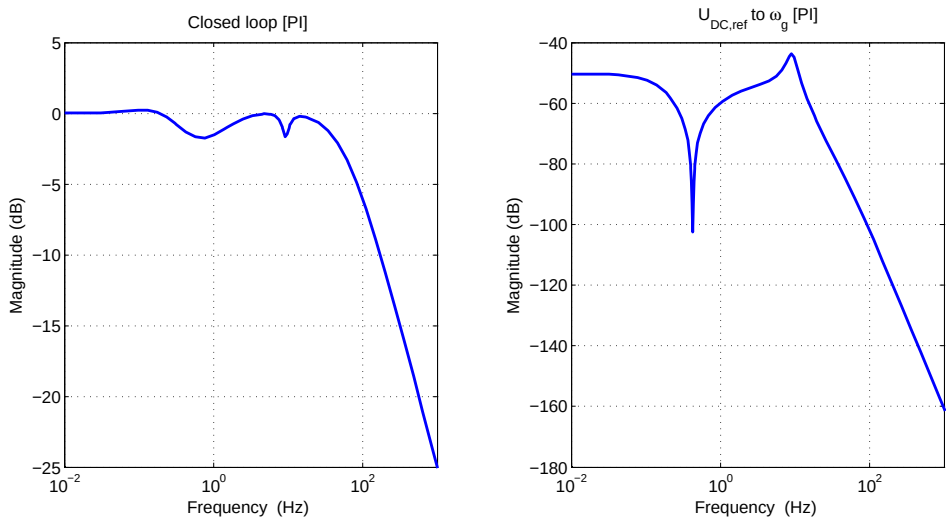

Figure 5.2: Transfer function of closed loop PI-controller, i.e. from $U_{DC,ref}$ to U_{DC}, to the left. To the right is the frequency response from $U_{DC,ref}$ to ω_g.

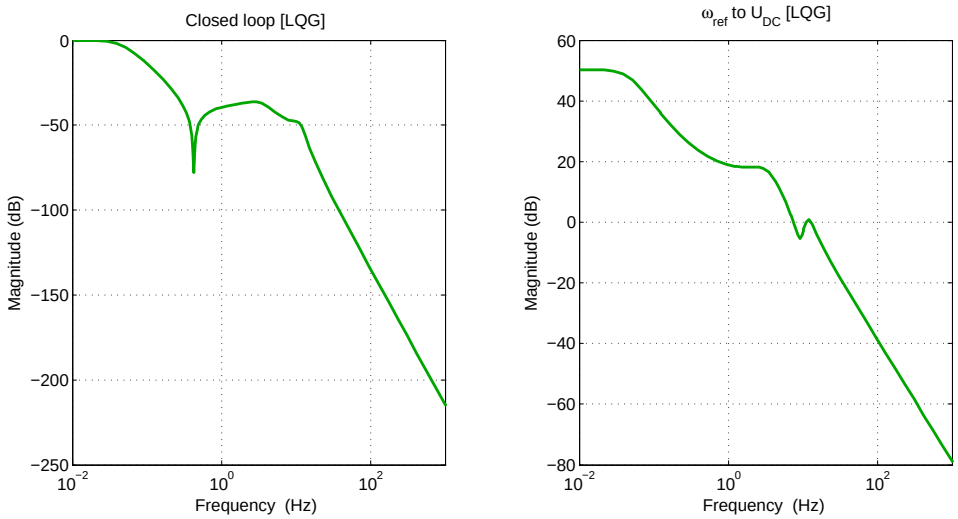

Figure 5.3: Frequency response of closed loop LQG-controller, i.e. from ω_{ref} to ω_g, to the left. To the right is the transfer function frequency response of ω_{ref} to U_{DC}.

Both transfer functions shows that the input sensitivity function goes to zero for low frequencies, i.e. there are some integral action in both controllers making the control error go to zero for constant disturbances.

One interesting thing to note about Figure 5.4 is that the LQG controller does not go asymptotically to zero for constant disturbances, as the PI controller does. This indicates that there is something wrong with the integral action in the LQG controller. The reason is that the filter included into the controller, to make the controller less sensitive to oscillations of about 50 Hz, counteracts the integral action. If the filter would be disregarded or given less energy in the Kalman filter, the LQG controller would exhibit a similar asymptotic behavior as the PI controller does.

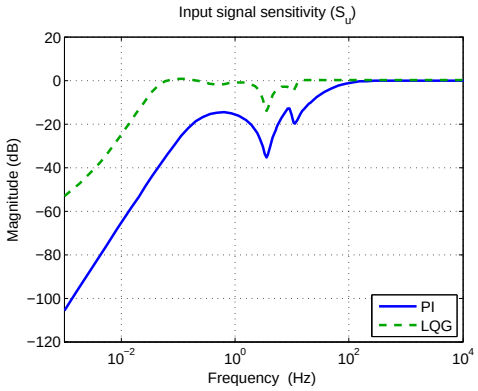

Figure 5.4: Input sensitivity function for the PI and LQG controller.

5.2.3 Disturbance in I_{out}

Figure 5.5 shows the effect of a disturbance in I_{out}. The peak at 9 Hz for the PI controller indicates that the disturbance will cause some oscillations, though they would be damped. The LQG controller does not have the same peak and hence one can expect less oscillations using that controller.

One can also see that the frequency response goes to zero for the PI controller, both for U_{DC} and ω_g, for low frequency disturbances in I_{out}. The same cannot be said for the LQG controller, meaning that the LQG controller cannot completely remove constant disturbances in I_{out}. The reason is that the filter for the complimentary sensitivity function interacts with the integral action of the controller. Without the filter the controller exhibits the same asymptotic behavior as the PI controller.

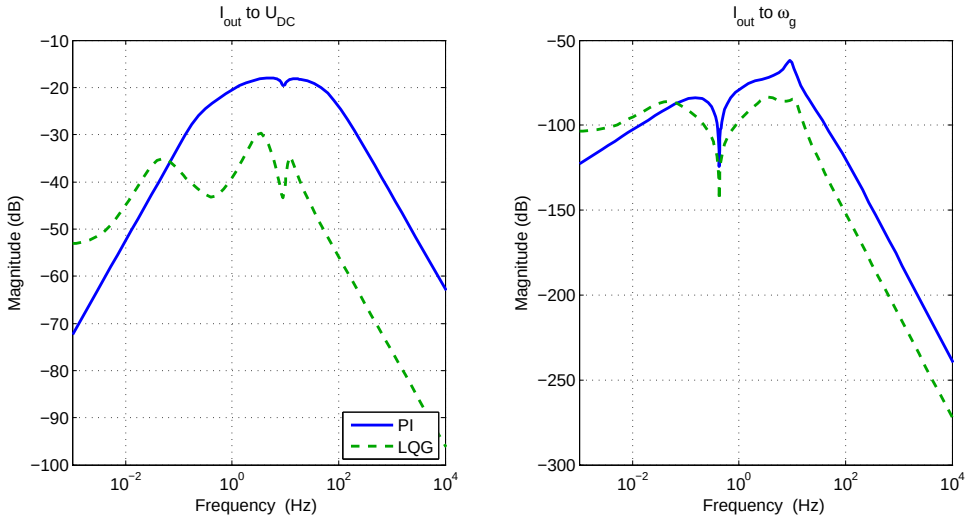

Figure 5.5: Frequency response of a disturbance in I_{out}.

5.3 Time domain simulations

The time domain simulations were first performed with a step in the reference signal, and then as a disturbance in I_{out}.

5.3.1 Step response

The LQG regulator was tuned such that it would manage to handle a step response without causing any oscillations whereas the PI regulator was tuned such that it would follow the reference voltage fast and accurate. The time domain simulations show that the DC voltage follows the reference value well at the cost of oscillations in the generator (Figure 5.6 and 5.7). The LQG controller slowly increases the voltage and without causing any oscillations.

According to Figure 5.2 and 5.3 the LQG controller has a much lower bandwidth than the PI controller, thus the LQG controller would be expected to react slower on changes in the reference signal. This is in agreement with the time domain simulations (Figure 5.6 and 5.7).

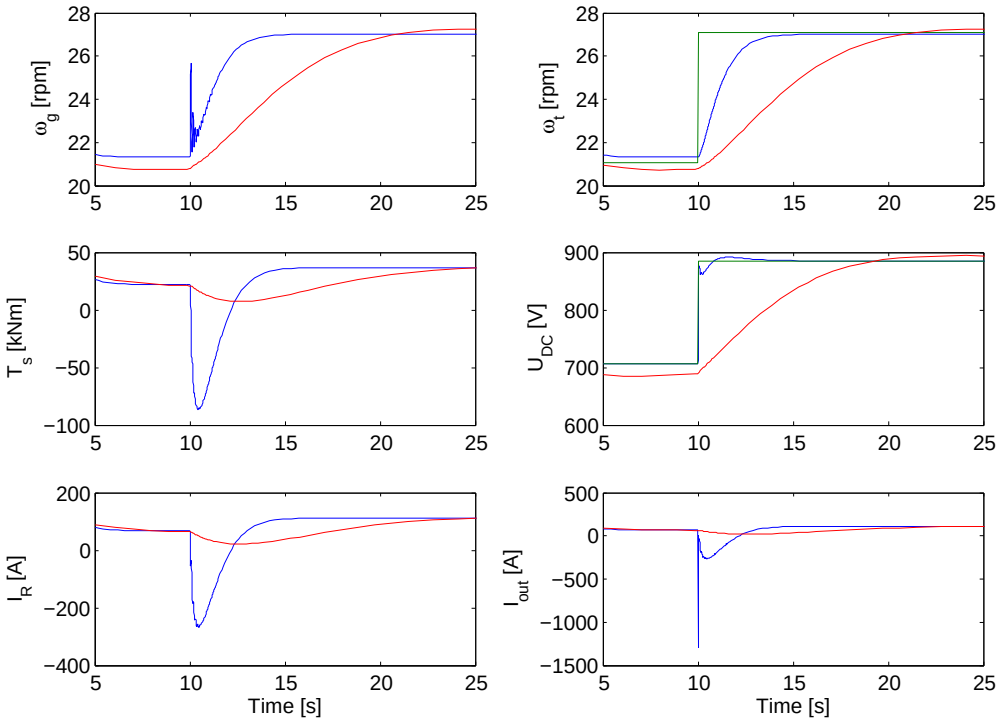

Figure 5.6: Response of PI (blue) and LQG (red) controller when reference signal (green) is changed in a step, simulated using equations (4.3) without limitations on I_R and U_{DC}, i.e. the result one would expect from the frequency response in Figure 5.2 and 5.3.

5.3.2 Disturbance response

Simulations with a disturbance in I_{out} (Figure 5.8) show that both controllers manage to handle the disturbance without being unstable or oscillating more than one period. The disturbance was simulated as a complete loss of I_{out} after 10 seconds lasting for 0.8 seconds, i.e. $I_{out} = 0$ in the interval. During that time the controllers did not have any controllability and could not do anything to stop the oscillations. This means that it is the behavior when the signal returns that is interesting to look at, i.e. the behavior after 10.8 seconds.

One can see in Figure 5.8 that the PI controller pushes down the DC voltage once the current is back. This causes the generator to oscillate down to about 11 rpm, and then back up again. The fast response causes big strains in the drive shaft and also high currents in both the inverter and the rectifier.

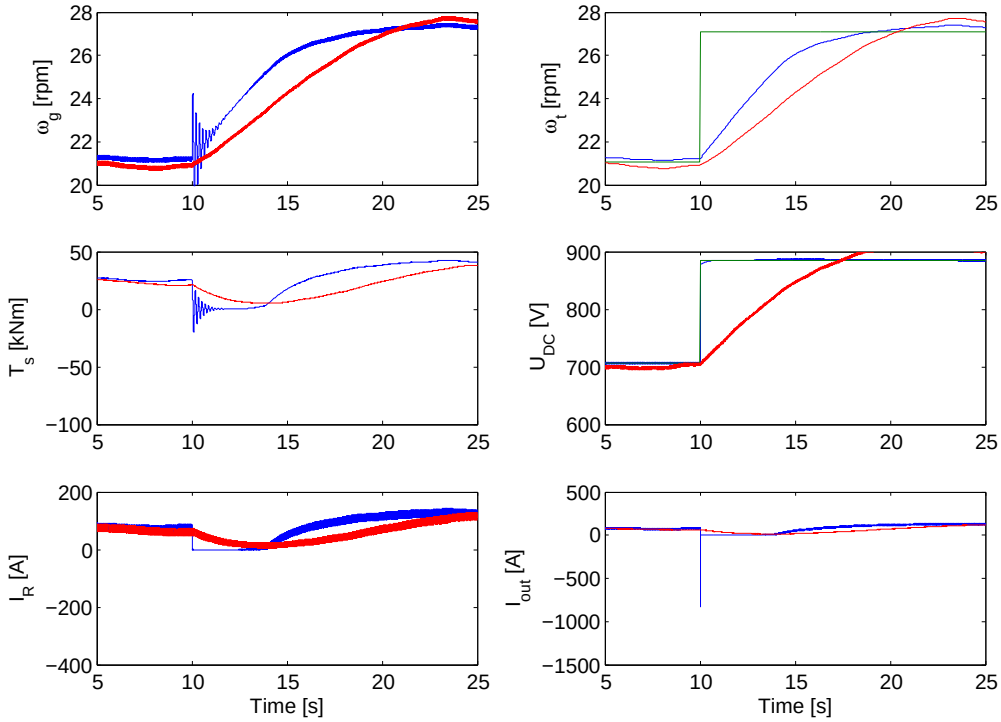

Figure 5.7: Response of PI (blue) and LQG (red) controller when reference signal (green) is changed in a step, simulated in MATLAB Simulink.

5.3.3 Kalman filter

Figure 5.9 illustrates the Kalman filter performance. One can note that there are oscillations in the true signal that does not reflect in the estimations. This is because of the filter that was included into the Kalman filter. The measured signals are ω_g, U_{DC} and I_R.

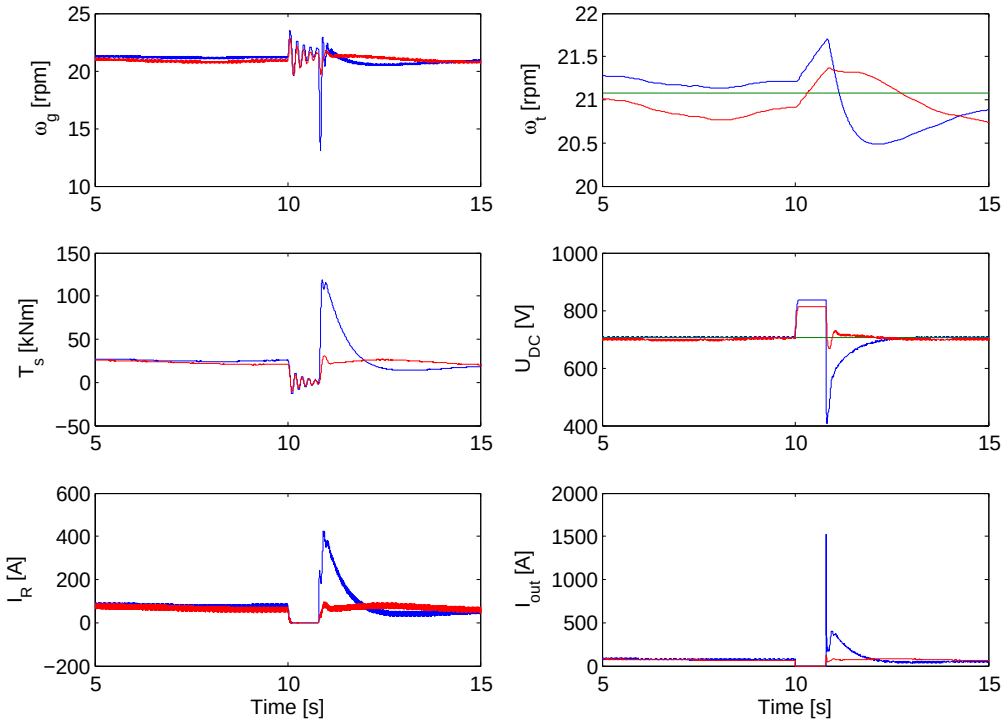

Figure 5.8: Disturbance response of PI (blue) and LQG (red) controller, simulated in MATLAB Simulink.

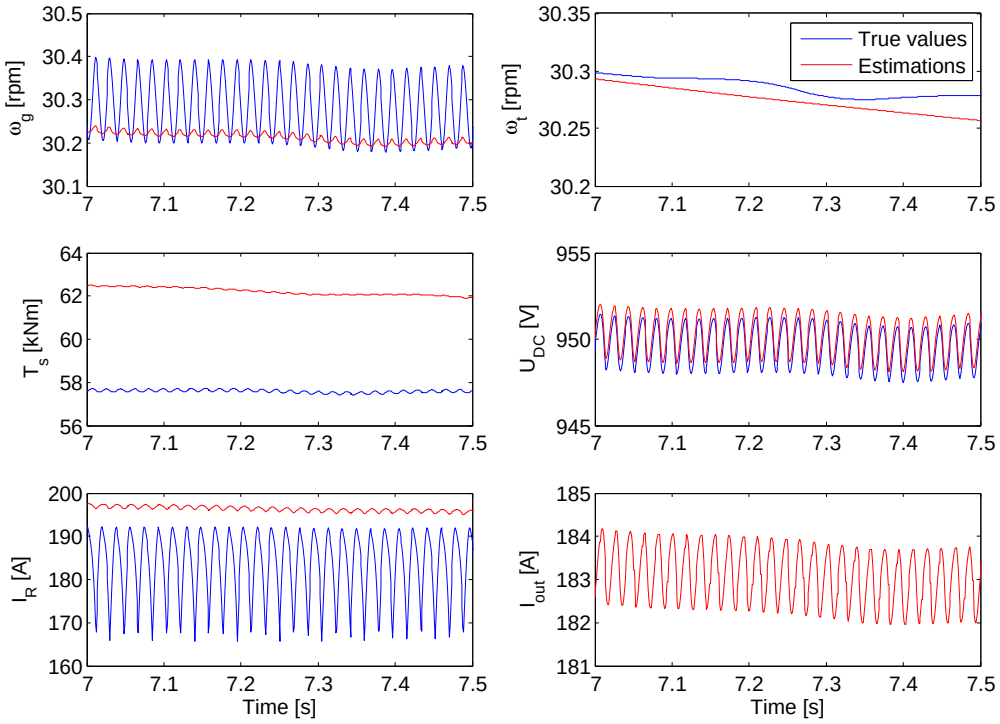

Figure 5.9: Difference between Kalman filter estimations and actual values of the state space variables, simulated in MATLAB Simulink.

Chapter 6

Discussion

Earlier studies have shown that direct driven permanent magnet generators easily excites oscillations in the drive train. As shown by [18] this is not the case for all types of configuration. In particular it is not a big issue neither with the PI controller nor with the LQG controller presented in this work. On the other hand there is a discussion whether or not this is an efficient way of extracting energy out of the wind.

6.1 LQG vs PI

There are advantages and disadvantages with both the PI controller and the LQG controller. The main advantage with the PI controller is that it is simple and manages to control the plant pretty well, whereas the LQG controller is more advanced and has the ability to not only keep the turbine at its reference speed but also to suppress torsional oscillations.

One of the greatest disadvantages with the LQG controller is that it does not make sure that the DC voltage does not vary too fast. If the DC voltage is varying too much it could affect the current controller and hence the dynamics of the input signal. However, this is of concern for the current controller and nothing that has been considered here.

6.1.1 Step response

The result seen in Figure 5.7 shows that the DC voltage is rapidly increased to its reference value using the PI controller, whereas the LQG controller is designed to slowly increase the voltage without causing any oscillations. The rapid increase in DC voltage from the PI regulator causes the generator to lose contact with the DC bus line because the voltage rises above the no load voltage of the generator and the saturation condition, $I_R \geq 0$, decouples the generator from the DC line. One easy way to avoid this decoupling is simply to limit the input signal, I_{out}, not to be less than zero, or by limiting the rate of change of the reference DC voltage. If the DC voltage is ramped up slowly it is possible to avoid the decoupling of the generator from the DC bus line.

One important thing to add to the discussion is that the reference signal is set on the basis of a 60 seconds running mean of the wind speed. This means that the reference signal is unlikely to change as fast as in a step, but will rather be much smoother. The only time the reference is changed in a step is when the turbine is supposed to accelerate through the eigenfrequencies of the tower, at startup.

6.1.2 Disturbance sensitivity

The LQG controller was designed to be less aggressive, i.e. slower. This is good because too much aggressiveness may cause problems in the drive train such as too much strain in the drive shaft. As seen in Figure 5.8 a drop in the PWM signal causes the DC voltage to rise quickly. Because the PI controller tries so hard to keep the DC voltage at its reference it causes big strains in the drive train and touches the limit of what the electrical and mechanical components can handle. This is not the case for the LQG controller, which is more gentle in some sense.

However, it is important to point out that the aggresiveness of the PI controller could be handled by an anti-windup function that limits the integral term in the PI controller in case of constant disturbances on the input signal. Using an anti-windup function would cause the PI controller to be less aggressive once the signal returns. An anti-windup function should also be included into the LQG controller in case of constant disturbances.

6.2 Energy capture

The both controllers use the same overall control strategy to capture the energy in the wind, i.e. a reference voltage/speed is set according to a look-up table for optimal power extraction. One might think that the LQG controller, which controls the rotational speed, would succeed better in keeping the tip speed ratio at its optimum and hence extract more power than the PI controller. However, if the look-up table for the DC voltage is carefully developed from experiments it is possible that also the voltage controller would be just as good.

The drawbacks of controlling the DC voltage, as the PI regulator does, is that the look-up table can never be made to perfectly fit the optimal rotational speed curve. This is because the relationship between the DC voltage and rotational speed is highly dependent on the power delivered from the wind. The available power in the wind is directly proportional to the density of air, which could be varying with about 20 %. This means that the DC voltage, set for a certain wind speed, would yield another rotational speed than it would do for the same wind speed with another air density.

6.3 Other solutions to the vibration problem

As described in the introduction there exist more than one way to optimize the energy capture from the wind. It is possible that Vertical Wind one day will try some other strategy than measuring the wind speed and keeping the DC-voltage at a constant reference value. Maybe there will be some restrictions from local grid owners that the active power should be smoothed out. According to [18] this could cause the system to oscillate and some dampening method would be necessary.

One way to handle the oscillations is to infer a torque that acts in the opposite direction of the oscillations. However, if the oscillations origins from the fact that the inverter cannot be controlled, e.g. grid fault or loss of PWM signal, it is useless to control the inverter to infer such a torque. The remaining solution is to exhaust power to an independent island operated resistive load such that the generator is damped. This method requires that the rotational speed of the generator is measured.

6.4 Reliability of the simulations

The shaft is modeled with the same equations and parameters as described by equations (2.4). This means that there is no difference between the mechanical model used for the Kalman filter and the real parts in the simulations. Because of the assumption that the shaft does not have any inertia it is possible that the true shaft will behave different than the one in the simulations. Another

possibility is that the shaft stiffness parameter, k_s, differs from the theoretical value, which has not been simulated.

The wind model simulates realistic wind speed fluctuations. The problem is that the reference speed/voltage is supposed to be set according to a moving average of the wind speed, which is not the case in the Simulink model. In the model the reference value is set according to a user defined mean value, which is a mean value of the current wind and not a moving average of the mean. To make the model even more realistic maybe it should be included into the model that the mast, measuring the wind, is located about 100 m away from the turbine, hence both time and direction would affect the correlation of reference speed and actual wind at the turbine.

The induced voltage of the generator was modeled as a trapezoidal function. The real shape of the generator voltage should differ from this simplification and it is hard to know what it will look like without further investigation. However, the effect of different subharmonics caused by the generator should have little impact on the outcome in reality.

The components of the electrical system can be assumed to be more or less correct modeled with SimPowerSystems toolbox. However, one can never know for sure the exact position and behavior of such components as inductances and resistances in the true system.

The simplification of replacing the inverter with a current source might seem coarse. The biggest drawback with this simplification is that the voltage over the DC line can be allowed to be less than the grid side voltage, U_{grid}, which is unrealistic. However, simulations have been made with a model that includes the inverter connected to the grid and the results indicate that this simplification is valid.

In the case of having an inverter connected to the grid instead of a current source there is a second control loop controlling the current, as described in section 3.2. If the LQG should be implemented correctly the dynamics of that controller should be included into the model. One suggestion is that it is included as

$$\dot{I}_{out} = \frac{1}{t_s}(I^*_{out} - I_{out}) + f(U_{DC})$$

where a suitable time constant, t_s, is set to describe the response of the controller and where I^*_{out} is the input current from the LQG controller and I_{out} is the actual current. The current also depends on the DC voltage, here described by the term $f(U_{DC})$. The very best should off course be to include the dynamics of the inverter into the model and to let the LQG regulator control the PWM signal.

6.5 Future work

The advantage of the LQG controller is that it, besides of being less aggressive, also includes state estimations of all the state variables using a Kalman filter. In this work it was assumed that there were three measurement signals: U_{DC}, I_R and ω_g. This is maybe unnecessary, maybe it would be enough to just measure one of the states, such as the DC voltage. That would also have made a better comparison between the LQG and the PI controller. However, the drawbacks of only measuring the DC voltage is that one can never be sure that the estimation of the rotational speed converges towards the true speed of the generator. Hence it is suggested that at least the rotational speed is measured. The performance of the Kalman filter could also be improved by adding a time constant to describe the dynamics of the current controller. Another improvement would be to replace the Kalman filter with an Extended Kalman filter to better estimate the nonlinear torque.

It would be interesting to investigate if the LQG controller could be developed further to optimize the energy capture of the turbine. This could be done by letting the Kalman filter estimate the wind speed, and hence set the reference value of ω_t. By doing so the turbine could be improved to follow the optimal tip speed ratio.

Another use of the Kalman filter could be to estimate the aerodynamic torque on the wings. If the estimated torque is exceedingly greater than expected from measurements of the wind speed

and the rotational speed one could expect that there would be ice on the wings. Ice on the wings is dangerous and the turbine should stop and get defrosted. So far there has been few successful suggestions of how to detect if there is any ice on the wings.

It would also be interesting to study if it would be possible to mitigate fatigue load fluctuations of the wings and the tower. This could be done by using measurements of the strain in the blades, similar to what has been done in [8]. However, it is important to point out that the configuration of the power electronics considered here infer some constraints that may limit the effectiveness of the regulator. Other suggestions of future work could be to compare the performance of the developed LQG controller with other controllers such as fuzzy control, sliding mode control or NMPC.

Chapter 7

Conclusions

This thesis has enlightened some of the improvements that can be done to the control system of a vertical axis wind turbine. A dynamical model has been developed that can be used for state space feedback control. The model was used for designing an LQG controller. The controller was designed to minimize a quadratic criterion that punishes both torsional oscillations, command following and input signal magnitude.

Torsional oscillations that occur because of disturbances on the input signal can not be damped by neither the PI controller nor the LQG controller. Hence, in case of a grid fault or loss of PWM signal, there is a need for some second control mechanism if dampening is required. A suggestion is to exhaust power to an independent island operated resistive load.

Though the LQG controller has been developed and seems to work properly in simulations it is important to point out that the existing PI controller handles torsional oscillations well. An implementation of the developed LQG controller might seem to be unnecessary. On the other hand it is possible that the LQG controller could be improved to take care of much more complicated design specifications than just torsional oscillations, such as maximizing the power output and minimizing oscillations in the wings and the tower.

Bibliography

[1] J. Ribrant and L. M. Bertling, "Survey of failures in wind power systems with focus on swedish wind power plants during 1997-2005," *IEEE Transactions on energy conversion*, vol. 22, no. 1, pp. 167–173, 2007.

[2] J. Manwell, J. McGowan, and A. Rogers, *Wind Energy Explained: Theory, Design and Application.* John Wiley and Sons Ltd, 2009.

[3] I. Munteanu, N. A. Cutululis, A. I. Bratcu, and E. Ceanga, "Optimization of variable speed wind power systems based on a LQG approach," *Control Engineering Practice*, vol. 13, pp. 903–912, 2005.

[4] P. Novak, T. Ekelund, I. Jovik, and B. Schmidtbauer, "Vibration Suppression in a Two-Mass Drive System Using PI Speed Controller and Additional Feedbacks - Comparative Study," *IEEE Control Systems*, vol. 15, no. 4, pp. 28–38, 1995.

[5] K. Szabat and T. Orlowska-Kowolska, "Vibration Suppression in a Two-Mass Drive System Using PI Speed Controller and Additional Feedbacks - Comparative Study," *IEEE Transactions on industrial electronics*, vol. 54, no. 2, pp. 1193–1206, 2007.

[6] S. Bolognani, A. Venturato, and M. Zigliotto, "Theoretical and experimental comparison of speed controllers for elastic two-mass-systems," in *Power Electronics Specialists Conference*, vol. 3, pp. 1087–1092, 2000.

[7] F. Lescher, H. Camblong, R. Briand, and R. Curea, "Alleviation of wind turbines loads with a LQG controller associated to intelligent micro sensors," in *Industrial Technology, 2006. ICIT 2006. IEEE International Conference on*, pp. 654 –659, 2006.

[8] S. Nourdine, H. Camblong, I. Vechiu, and G. Tapia, "Comparison of wind turbine LQG controllers using individual pitch control to alleviate fatigue loads," in *Control Automation (MED), 2010 18th Mediterranean Conference on*, pp. 1591 –1596, 2010.

[9] H. Vihriälä, *Control of variable speed wind turbines.* PhD thesis, Tampere University of Technology, 2002.

[10] F. Lescher, J. Y. Zhao, and A. Martinez, "LQG multiple model control of a variable speed, pitch regulated wind turbine," in *17th IMACS World Congress, Paris, France*, 2005.

[11] C. L. Bottasso, A. Croce, and B. Savini, "Performance comparison of control schemes for variable-speed wind turbines," *Journal of physics. Conference series*, vol. 75, p. 012079, 2007.

[12] D. Dang, Y. Wang, and W. Cai, "Nonlinear model predictive control (NMPC) of fixed pitch variable speed wind turbine," in *Sustainable Energy Technologies, 2008. ICSET 2008. IEEE International Conference on*, pp. 29 –33, 2008.

[13] I. Munteanu, S. Bacha, A. Bratcu, J. Guiraud, and D. Roye, "Energy-reliability optimization of wind energy conversion systems by sliding mode control," *Energy Conversion, IEEE Transactions on*, vol. 23, no. 3, pp. 975 –985, 2008.

[14] B. Boukhezzar and H. Siguerdidjane, "Nonlinear control with wind estimation of a DFIG variable speed wind turbine for power capture optimization," *Energy Conversion and Management*, vol. 50, pp. 885 –892, 2009.

[15] C. Jauch, "Transient and Dynamic Control of a Variable Speed Wind Turbine with Synchronous Generator," *Wind Energy*, vol. 10, pp. 247–269, 2007.

[16] G. Michalke, A. D. Hansen, and T. Hartkopf, "Control strategy of a variable speed wind turbine with multipole permanent magnet synchronous generator," in *European Wind Energy Conference*, 2007.

[17] A. D. Hansen and G. Michalke, "Modelling and Control of a Variable-speed Multi-pole Permanent Magnet Synchronous Generator Wind Turbine," *Wind Energy*, vol. 11, pp. 357–554, 2008.

[18] H. Geng, D. Xu, and G. Yang, "Comparison of oscillation damping capability in three power control strategies for PMSG-based WECS," *Wind Energy*, vol. 14, pp. 389–406, 2011.

[19] S. Eriksson and H. Bernhoff, "Generator-damped torsional vibrations of a vertical axis wind turbine," *Wind Energy*, pp. 449–462, 2005.

[20] T. L. Skvarenina, *The Power Electronics Handbook, chapter 7.* CRC Press, 2001.

[21] M. Chinchilla, S. Arnaltes, and J. C. Burgos, "Control of permanent-magnet generators applied to variable-speed wind-energy system connected to the grid," *IEEE Transactions on energy conversion*, vol. 21, no. 1, pp. 130–135, 2006.

[22] J.-K. Ji and S.-K. Sul, "Kalman Filter and LQ Based Speed Controller for Torsional Vibration Suppression in a 2-Mass Motor Drive System," *IEEE Transactions on industrial electronics*, vol. 42, no. 6, pp. 564–571, 1995.

[23] T. Glad and L. Ljung, *Reglerteori, flervariabla och olinjära system.* Studentlitteratur, 2003.

[24] Mathworks, "MATLAB R2011b documentation: Control system toolbox, kalmd," 2011.

Appendix A

Simulink model - LQG

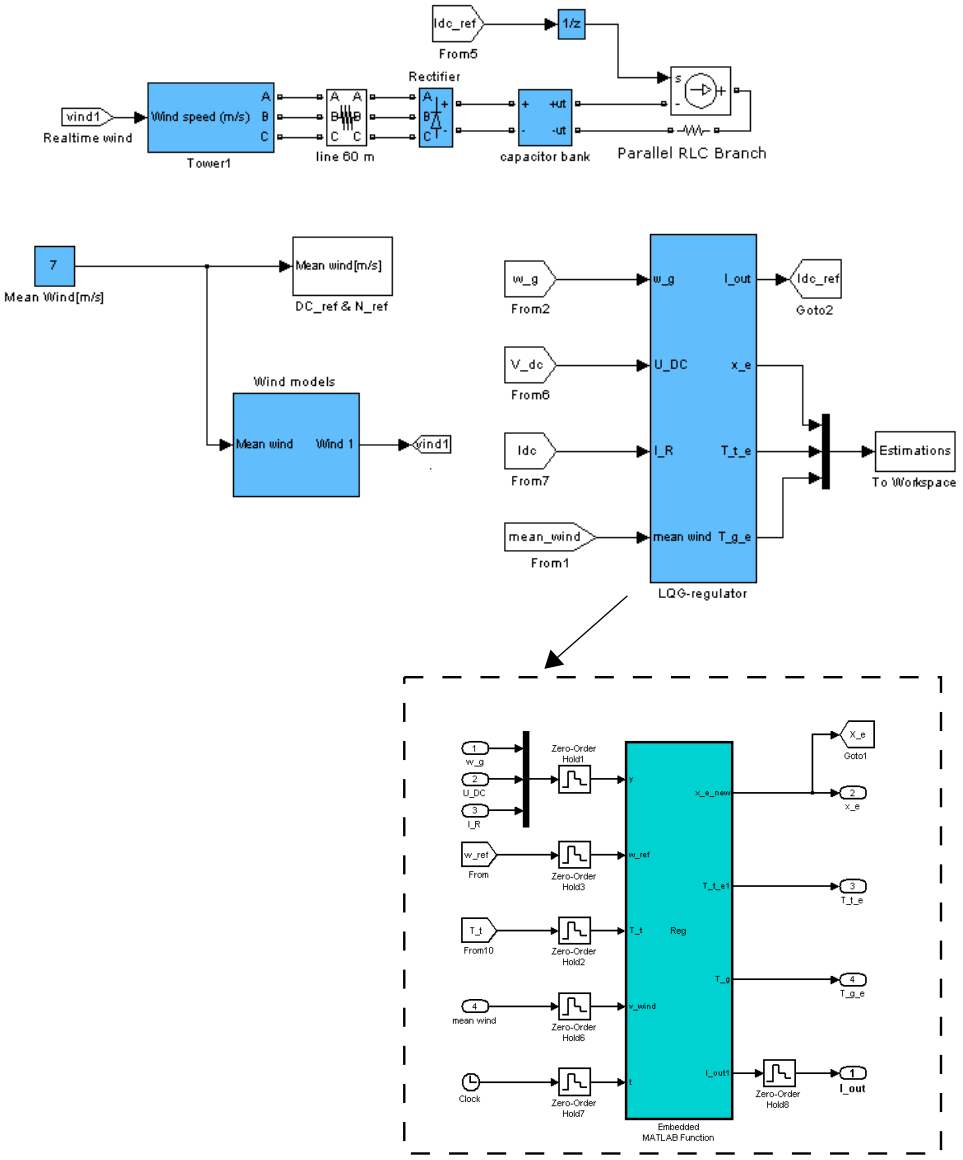

Appendix B

Computations in the regulator

Defining variables:

- R = radius of turbine = 13 m
- H = height of turbine = 24 m
- ρ = air density = 1.2 kg/m^3
- v_{wind} = 60 s running mean of the wind speed

State variables and meassurements:

$$x_e = \begin{bmatrix} \hat{\omega}_g & \hat{\omega}_t & \hat{T}_s & \hat{U}_{DC} & \hat{I}_R & \Delta\hat{T}_t & \dot{\hat{\tau}}_g & \hat{\tau}_g & \dot{\hat{\varepsilon}} & \hat{\varepsilon} \end{bmatrix}^T$$

$$y = \begin{bmatrix} \omega_g & I_R & U_{DC} \end{bmatrix}^T$$

Get ω_{ref} from lookup table:

$$\omega_{ref} = \text{interp1}(\omega_{ref}(v_{wind}))$$

Calculate torque:

$$\lambda = \frac{x_e(2)R}{v_{wind}}$$
$$C_{P,ref} = \text{interp1}(C_P(\lambda))$$
$$T_{t,e} = C_{P,ref}\frac{\rho R H v_{wind}^3}{x_e(2)}$$

Calculate I_{out}:

$$I_{out} = -L\begin{bmatrix} x_e \\ \epsilon \end{bmatrix}$$

Chose which Kalman filter to use:

$$
\begin{aligned}
y0 &= \begin{bmatrix} 18 & 18 & 18 \end{bmatrix} \\
x0 &= \begin{bmatrix} 7.3 & 11.5 & 15.5 \end{bmatrix} \\
y1 &= \begin{bmatrix} 32.8 & 32.9 & 32.9 \end{bmatrix} \\
x1 &= \begin{bmatrix} 14.8 & 19.2 & 22.9 \end{bmatrix} \\
k &= \frac{y0 - y1}{x0 - x1} \\
f_i &= k_i(v_{wind} - x0_i) + y0_i; \quad i = 1, 2, 3 \\
\omega_t &= x_e(2)\frac{30}{\pi}
\end{aligned}
$$

$$
K = \begin{cases} K_1 & \text{if} \quad f_1(v_{wind}) < \omega_t \\ K_2 & \text{if} \quad f_2(v_{wind}) < \omega_t < f_1(v_{wind}) \\ K_3 & \text{if} \quad f_3(v_{wind}) < \omega_t < f_2(v_{wind}) \\ K_4 & \text{if} \quad \omega_t \leq f_3(v_{wind}) \end{cases}
$$

Update the states:

$$
\begin{bmatrix} x_e \\ \epsilon \end{bmatrix} = \begin{bmatrix} F & 0 \\ 0 & 1 \end{bmatrix} \begin{bmatrix} x_e \\ \epsilon \end{bmatrix} + \begin{bmatrix} G & H \\ 0 & 0 \end{bmatrix} \begin{bmatrix} I_{out} \\ T_{t,e} \end{bmatrix} + \begin{bmatrix} K \\ 0 \end{bmatrix} (y - Cx_e) + \begin{bmatrix} 0 \\ dt \end{bmatrix} (x_e(2) - w_{ref})
$$

Send I_{out} to current regulator, hold for dt, and start over again.